

Effect of Hydrophobic Chain Length of Amphiphilic Silicone Oil (Copolymer) on the Nonionic Surfactant-Layer Curvature

Masaya Kaneko,[†] Katsutoshi Matsuzawa,[†] Md. Hemayet Uddin,^{†,‡}
M. Arturo López-Quintela,[§] and Hironobu Kunieda[†]

Graduate School of Environment and Information Sciences, Yokohama National University, Tokiwadai 79-7, Hodogaya-ku, Yokohama 240-8501, Japan, Department of Applied Chemistry and Chemical Technology, Islamic University, Kustia, Bangladesh, and Departamento de Química Física, Facultad de Química, Universidad de Santiago de Compostela, E-15782 Santiago de Compostela, Spain

Received: February 3, 2004; In Final Form: June 22, 2004

Phase behavior and formation of self-assemblies in ternary water/ penta(oxyethylene) dodecyl ether (C_{12} -EO₅)/amphiphilic silicone copolymer, poly(dimethylsiloxane)–poly(oxyethylene) ($Si_mC_3EO_{3.2}$) systems, were investigated. These silicone copolymers are very hydrophobic because of the short EO chain and are essentially water-insoluble amphiphilic oils, similar to high alcohols or fatty acids. In general, the surfactant layer curvature becomes less positive upon addition of amphiphilic oils, similar to what happens with high alcohols or fatty acids. This is what is observed for $m = 5.8$. However, in the ternary water/ C_{12} EO₅/ $Si_{25}C_3EO_{3.2}$ system, the surfactant layer curvature becomes more positive, and micellar cubic, normal hexagonal, and bicontinuous cubic phases are also formed, although a lamellar liquid crystal forms only in the water– C_{12} EO₅ system. In the liquid crystal regions, it was found that $Si_{25}C_3EO_{3.2}$ is not dissolved in the thin bilayer of the C_{12} EO₅ lamellar phase, whereas the long and bulky $Si_{25}C_3$ chain forms an oil core in those cubic, hexagonal, and bicontinuous cubic phases, in which the surfactant is absorbed at the hydrophobic interface of each aggregate. Then, this opposite effect of added amphiphilic silicone copolymer or oil to the surfactant solution is attributed to the long and flexible $Si_{25}C_3$ chain which makes an oil pool inside the aggregates. This different behavior of small and large Si_mC_3 chains is also observed in the cloud temperatures. In fact, the cloud temperature of C_{12} EO₅ aqueous solution decreases upon addition of $Si_{5.8}C_3EO_{3.2}$, whereas it increases by adding a long hydrophobic chain, like $Si_{14}C_3EO_{3.2}$ or $Si_{25}C_3EO_{3.2}$ silicone oil. It was confirmed by DLS that long rod micelles, which are present in the water– C_{12} EO₅ system, become small spherical micelles upon addition of $Si_{25}C_3EO_{3.2}$. Consequently, hydrophobic $Si_mC_3EO_{3.2}$ changes the micellar shape in two different ways depending on the length of the Si_mC_3 chain. For small chains (e.g., $m = 5.8$), the surfactant–copolymer layer curvature changes to less positive by forming a mixed layer. Long and bulky chains (e.g., $m = 14, 25$) make an oil core and this tends to make the curvature more positive, being this effect pronounced with increasing the hydrophobic chain length.

Introduction

Surfactant self-organized structures and/or surfactant layer curvatures are highly affected by solubilized oils. Aromatic hydrocarbons or long-chain aliphatic alcohols tend to be solubilized in the surfactant palisade layer and make the surfactant layer curvature negative or less positive,^{1–3} where the positive curvature means that the interface is convex toward water. Hence, a normal hexagonal to lamellar (rod-bilayer) phase transition takes place upon addition of amphiphilic oils. On the other hand, long-chain saturated hydrocarbons are solubilized in the deep inside of surfactant aggregates making an oil pool in the micelles.^{2,3} To minimize the surface area or contact between the polar and apolar parts, the surfactant layer curvature of the aggregates changes to more positive, and as a result, a rod-sphere transition takes place upon addition of hydrocarbon.^{4–8} In fact, although a micellar cubic (I_1) phase is not formed in many hydrophilic surfactant aqueous systems, the I_1 phase is

produced from a hexagonal (H_1) phase upon addition of a small amount of long hydrocarbon.^{2,3,9,10}

It is also well-known that cloud temperature of poly(oxyethylene)-type nonionic surfactant aqueous solution decreases in the presence of amphiphilic oils or aromatic hydrocarbons,³ whereas it increases upon addition of long-chain hydrocarbons.³ To our knowledge, there is no report on the increase in cloud temperature of nonionic surfactant solution upon addition of amphiphilic oils. However, the carbon number of amphiphilic oil is usually limited in the range of C_6 – C_{18} because the melting point of higher alcohols or fatty acids is too high to be solubilized in surfactant aggregates at room temperature. The melting temperature of long-chain hydrocarbons also increases with the increase in carbon number. If a solubilize is in a solid state, we have to consider additional factors for solubilization, such as melting enthalpy and entropy. On the other hand, silicone oil, poly(dimethylsiloxane) has a very flexible chain and even polymers of high molecular weight are in a liquid state due to their low cohesive energy.^{11,12} If a long silicone chain with a short hydrophilic chain is solubilized in surfactant aggregates, we could understand how the bulky-

* To whom correspondence should be addressed.

[†] Yokohama National University.

[‡] Islamic University.

[§] Universidad de Santiago de Compostela.

hydrophobic chains of amphiphilic solubilizes influences the surfactant layer curvature.

The phase behaviors of the mixture of large A–B type nonionic block copolymers and small nonionic surfactants in water were already reported.^{13–15} In these systems, the so far used nonionic block copolymers have hydrophilic chains long enough to form a self-organized structure at room or high temperatures as is similar to the large “surfactant” molecules. On the contrary, the block copolymers studied in this experiment are essentially “oil”, in other words, they do not have ability to form any self-organized structures. Therefore, it cannot be expected that the observed interesting phenomena, as for example, the formation of a variety of self-organized structures and the increase of the cloud temperature of surfactant aqueous solutions upon addition of a hydrophobic copolymer take place.

In this context, we investigated the phase behavior of a hydrophilic–lipophilic balanced nonionic surfactant, C₁₂EO₅, with an amphiphilic silicone oil (copolymer) having a short EO chain in water. The correlation between the cloud temperature and the micellar shape is also discussed.

Experimental Section

Materials. Poly(dimethylsiloxane)–poly(oxyethylene) diblock copolymers or amphiphilic silicone oils (Si_mC₃EO_{3.2}) are linear block copolymers were kindly synthesized by Dow Corning-Toray Co Ltd., Japan, where *m* is the number of dimethylsiloxane units. C₃ means a propylene residue connecting hydrophobic and hydrophilic chains. Since they have a very short EO chain, the silicone copolymers are fluid, transparent, and insoluble in water. Therefore, they behave essentially as silicone oils. The purities are 97.9% for Si₂₅C₃EO_{3.2}, 99.5% for Si₁₄C₃EO_{3.2}, and 78.2% for Si_{5.8}C₃EO_{3.2}. The impurity of the sample is mainly unreacted poly(oxyethylene). The polydispersity indices, *M_w*/*M_n*, are 1.20 for Si₂₅C₃, 1.19 for Si₁₄C₃, and 1.02 for Si_{5.8}C₃ chain and 1.21 for the poly(oxyethylene) (EO_{3.2}) chain, confirmed by gel permeation chromatography. Homogeneous penta-(oxyethylene)–dodecyl ether (C₁₂EO₅) were obtained from Nikko Chemicals Co., Japan.

The molar volumes of copolymers and surfactant, which were determined by the densitometer (Anton Paar 40),¹⁶ are 2118 cm³ for Si₂₅C₃EO_{3.2}, 1270 cm³ for Si₁₄C₃EO_{3.2}, 629 cm³ for Si_{5.8}C₃EO_{3.2}, and 418 cm³ for C₁₂EO₅. It is known that arithmetic addition holds concerning the molar volumes of each functional group in the surfactant.^{17,18} The molar volume of the hydrophobic part is calculated by extrapolating the molar volume of the total amphiphile, Si₂₅C₃EO_n, Si₁₄C₃EO_n or Si_{5.8}C₃EO_n having different poly(oxyethylene) chain lengths. Besides, the molar volume of the poly(oxyethylene) surfactant is proportional to *n*. The slope corresponds to the molar volume of 1 EO chain, 38.8 cm³/mol.^{2,19} The volume fractions of the hydrophilic part in the total amphiphile, *f*, are 0.06 for Si₂₅C₃EO_{3.2}, 0.1 for Si₁₄C₃EO_{3.2}, 0.21 for Si_{5.8}C₃EO_{3.2}, and almost 0.5 for C₁₂EO₅, where the values of hydrophobic parts are 215 cm³/mol or 0.357 nm³/molecule for C₁₂-,² and 1985 cm³/mol or 3.29 nm³/molecule for Si₂₅C₃-,¹⁶ 1137 cm³/mol or 1.89 nm³/molecule for Si₁₄C₃- and 504 cm³/mol or 0.84 nm³/molecule for Si_{5.8}C₃-. All compounds were used without further purification. Throughout this study Millipore water was used.

Phase Diagrams. The phase boundaries were determined by titrating mixtures of surfactant and copolymer with water at various mixing fractions. To confirm each phase boundary, some samples were made individually in sealed glass vials. Samples were kept at room temperature (~25 °C) for several weeks to months depending on their stability. The sample appearance was

not changed for at least 3 months. Phase equilibria were determined by visual observation of the samples and also observed through cross polarizers for anisotropy.

Calculation of the Volume Fraction of the Hydrophobic Part of Amphiphiles. The volume fraction of the hydrophobic part of amphiphiles (surfactant or copolymer) was calculated by the following equation:

$$\phi_L = \frac{V_L}{V_S + \frac{M_S}{\rho_w} \frac{1 - W_S}{W_S}} \quad (1)$$

where *V_S* and *V_L* are the molar volumes of the amphiphile and its hydrophobic moiety. *M_S* is the molecular weight of the amphiphile. *ρ_w* is the density of water. *W_S* is the weight fraction of the amphiphile in the water-amphiphile system. In the calculations of the mixed amphiphile system, we assumed the following equation:

$$\overline{V_S} \text{ or } \overline{V_L} \text{ or } \overline{M_S} \text{ or } \overline{a_S} = Y_1 X_1 + Y_2 X_2 \quad (2)$$

where *X₁* and *X₂* are mole fractions and *Y₁* and *Y₂* are intensive properties of copolymer and surfactant, respectively.

Small-Angle X-ray Scattering (SAXS). The types of liquid crystals formed were confirmed by using SAXS, performed on Rigaku Nano Viewer, which is equipped with a confocal mirror and CCD detector. X-ray power is 0.8 kW. All measurements were carried out at 25 °C. The samples were covered by plastic films for the SAXS experiments (Mylar seal method). To analyze the detailed structures of each liquid crystal, we measured interlayer spacings, *d*, of I₁, H₁, V₁, and L_α phases. The identification of cubic structures (I₂ and V₂ phases) is discussed in detail in a later section. According to geometrical relations, the following equations hold for the interlayer spacing, *d*, and the volume fraction of hydrophobic part of amphiphile, *φ_L*, for each liquid crystal.

For the I₁ phase

$$d = (36\pi)^{1/3} \frac{n_m^{1/3}}{\sqrt{h^2 + k^2 + l^2}} \frac{V_L}{a_S} \left(\frac{1}{\phi_L} \right)^{1/3} \quad (3)$$

For the H₁ phase

$$d = (2\sqrt{3}\pi)^{1/2} \frac{V_L}{a_S} \left(\frac{1}{\phi_L} \right)^{1/2} \quad (4)$$

where *a_S* and *V_L* are the effective cross sectional area and the volume of the hydrophobic part in the amphiphile, respectively. *n_m* is the number of micelles in a unit cell. *h*, *k* and *l* are Miller indices. For instance, *n_m* and *h² + k² + l²* are 1 and 1 for the Pm3m cubic structure.

Dynamic Light Scattering (DLS). DLS measurements were performed with a DLS-7000 (Otsuka Electronics Co., Ltd.) equipment. DLS apparatus consists of a goniometer, a 10 mW He–Ne laser (λ = 632.8 nm) and a Multiple Tau Digital Real Time Correlator (ALV-5000/EPP, Germany). The intensity correlation function, *g₂(t)*, was measured

$$g_2(t) - 1 = \beta |g_1(t)|^2 \quad (5)$$

where *g₁(t)* is the field correlation function, which is fitted by the regularization CONTIN program. When aggregates of different sizes are formed in solution, *g₁(t)* includes all of

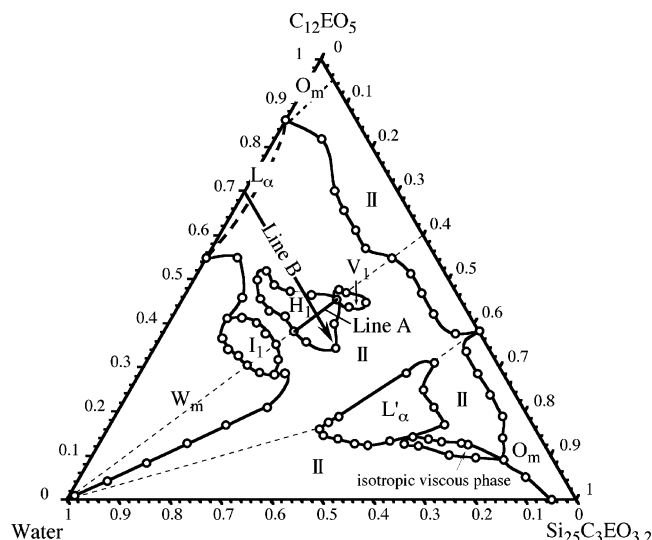


Figure 1. Ternary phase diagram of the water/ $C_{12}EO_5$ / $Si_{25}C_3EO_{3.2}$ system at 25 °C. I_1 : micellar cubic liquid crystalline phase, H_1 : hexagonal liquid crystalline phase, V_1 : bicontinuous cubic liquid crystalline phase, L_α or L'_α : surfactant-rich or copolymer-rich lamellar liquid crystalline phase and O_m : reverse micellar or surfactant liquid phase, II: two-phase region.

the individual relaxation processes and can be expressed as follows:²⁰

$$\sqrt{g_2(t) - 1} = \sqrt{\beta} \int_0^\infty A(\Gamma) e^{-\Gamma t} d\Gamma \quad (6)$$

where β is an adjusted parameter depending on the performance of the instrument, $A(\Gamma)$ is the relaxation rate distribution function and Γ is the relaxation rate given by eq 7

$$\Gamma = q^2 D \quad (7)$$

where D is the diffusion coefficient and q is the scattering vector amplitude given by eq 8

$$q = \frac{4\pi n}{\lambda_0} \sin\left(\frac{\theta}{2}\right) \quad (8)$$

n is the refractive index of the solvent, λ_0 is the laser beam wavelength, and θ is the scattering angle. The effective diffusion coefficient, D_{eff} , for spherical particles, is related to the apparent hydrodynamic radius, R_H^{app} , by the Stokes–Einstein equation

$$D_{\text{eff}} = \frac{k_B T}{6\pi\eta_0 R_H^{\text{app}}} \quad (9)$$

where k_B is the Boltzmann constant, T is the absolute temperature, and η_0 is the viscosity of water (890.9 $\mu\text{Pa s}$).

The q^2 dependence predicted by eq 7 was checked by performing the experiments at 5 different scattering angles (45°, 60°, 75°, 90°, and 110°). The R_H^{app} values reported are the average values obtained for the different angles. All of the measurements were made at 25 °C. All samples were kept at room temperature for at least 1 week before performing the DLS measurements.

Results and Discussions

Phase Behavior of $C_{12}EO_5$ + $Si_{25}C_3EO_{3.2}$ in Water. The ternary phase diagram of water/ $C_{12}EO_5$ / $Si_{25}C_3EO_{3.2}$ system at 25 °C is shown in Figure 1. $C_{12}EO_5$ forms an aqueous micellar solution (W_m), a lamellar liquid crystalline (L_α) phase, and a

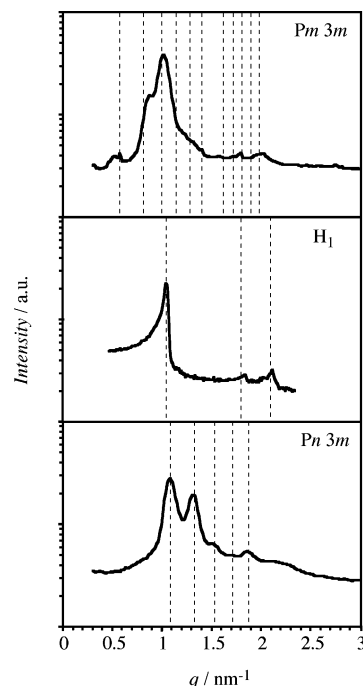


Figure 2. SAXS diffraction patterns of I_1 phase ($Pm\bar{3}m$), H_1 phase and V_1 phase ($Pn\bar{3}m$) in water/ $C_{12}EO_5$ / $Si_{25}C_3EO_{3.2}$ system at 25 °C. The broken lines correspond to the Miller indices for $Pm\bar{3}m$ space group, (100), (110), (111), (200), (210), (211), (220), (300/221), (310), (311), and (222), those for hexagonal peaks (100), (111), and (200), and those for $Pn\bar{3}m$ space group, (110), (111), (200), (210), and (211), respectively.

surfactant liquid (O_m), successively. A two-phase region is denoted by II. Although the hexagonal liquid crystalline (H_1) and the bicontinuous cubic liquid crystalline (V_1) phases are formed in the water– $C_{12}EO_5$ system, their melting temperatures are lower than 25 °C,^{21,22} and they do not appear in the phase diagram.

$Si_{25}C_3EO_{3.2}$ is essentially an amphiphilic oil which is not soluble in water. In a wide range of the binary water– $Si_{25}C_3EO_{3.2}$ system (the bottom axis in Figure 1), only immiscible two liquid phases are observed. $Si_{14}C_3EO_{3.2}$ and $Si_{5.8}C_3EO_{3.2}$ are also insoluble in water. However, a large amount of $Si_{25}C_3EO_{3.2}$ is incorporated in $C_{12}EO_5$ aqueous solution (W_m) as is shown in Figure 1. There should be III phase region between II phase regions in this phase diagram. However, III phase region is omitted because it is very narrow and out of point in this text. Since only less than 0.25 wt % poly(dimethylsiloxane) oil (Si_{16}) without a hydrophilic chain is solubilized in 30 wt % $C_{12}EO_5$ aqueous solution, the short EO chain is crucial for a large solubilization. In the ternary system, micellar cubic liquid crystal (I_1), H_1 and V_1 phases are formed being their layer curvatures more positive than those in the L_α phase, although a hydrophobic amphiphile, $Si_{25}C_3EO_{3.2}$, is added to the balanced surfactant solution.

The SAXS diffraction patterns for the I_1 , H_1 , and V_1 phases are shown in Figure 2. The reciprocal interlayer spacing ratios, $1:\sqrt{2}:\sqrt{3}:\sqrt{4}:\sqrt{5}:\sqrt{6}:\sqrt{8} \cdots$ for the I_1 phase, $1:\sqrt{3}:\sqrt{4} \cdots$ for the H_1 phase, and $\sqrt{2}:\sqrt{3}:\sqrt{4}:\sqrt{5}:\sqrt{6} \cdots$ for the V_1 phase are indicated by broken lines in Figure 2. From the obtained peak ratios, probably, the I_1 phase belongs to the $Pm\bar{3}m$ and the V_1 phase belongs to the $Pn\bar{3}m$ structures (OBDD; ordered bicontinuous double-diamond).^{23,24}

Figure 3 shows the square of interlayer spacing, d^2 , as a function of the reciprocal of the volume fraction of hydrophobic part in the H_1 phase of $Si_{14}C_3EO_{3.2}$ – $C_{12}EO_5$ and $Si_{25}C_3EO_{3.2}$ –

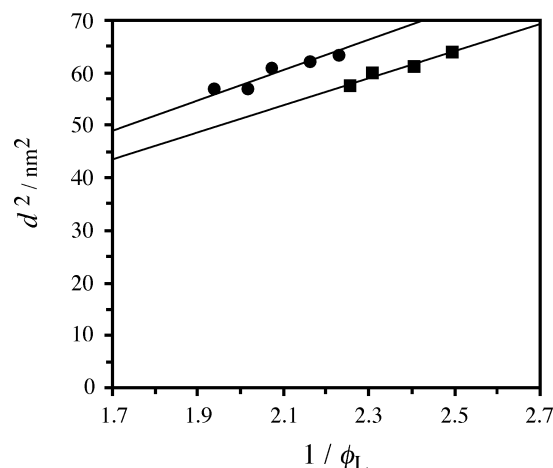


Figure 3. Square of interlayer spacing, d^2 , as a function of the reciprocal of ϕ_L at $W_1 = 0.4$ at 25 °C. ●; $\text{Si}_{25}\text{C}_3\text{EO}_{3.2}$ system, ■; $\text{Si}_{14}\text{C}_3\text{EO}_{3.2}$ system.

C_{12}EO_5 systems, at constant mixing fraction of the copolymer in the total amphiphile, $W_1 = 0.4$ (line A in Figure 1) at 25 °C. The d^2 value for H_1 phase monotonically increases with the increase in water content (decreases in W_S) as indicated by eq 4. This means that the cylindrical rod micelles remain unchanged during the dilution and only the distance between them is increased. The average cross sectional areas, $\overline{a_s}$, are calculated to be 0.41 nm² for the $\text{Si}_{14}\text{C}_3\text{EO}_{3.2}$ system and 0.43 nm² for the $\text{Si}_{25}\text{C}_3\text{EO}_{3.2}$ system. Since the mole fraction of C_{12}EO_5 in the mixture is around 0.8, the $\overline{a_s}$ for both systems are similar, because the surfactant cross sectional area is mainly reflected on $\overline{a_s}$. The radii of the hydrophobic part of the rod micelles in the H_1 phase are 3.1 nm for the $\text{Si}_{14}\text{C}_3\text{EO}_{3.2}$ system and 3.3 nm for the $\text{Si}_{25}\text{C}_3\text{EO}_{3.2}$ system, and are much longer than the hydrophobic chain length of C_{12}EO_5 in its extended state (1.67 nm).¹⁸ Hence, the long and flexible Si_mC_3 - chain makes an oil pool inside the rod micelles. Although the Si_{25}C_3 -chain is more than 1.5 times larger than the Si_{14}C_3 -chain, both radii are not very different. The reason being that a long and flexible polymer chain tends to be in a bulky state because the extended state is entropically unfavorable.

In the $\text{Si}_{25}\text{C}_3\text{EO}_{3.2}$ -rich region, an anisotropic copolymer-rich, L'_α and an isotropic viscous phase are observed. L'_α phase is a lamellar structure confirmed by its polarized microscopic pattern. The isotropic and highly viscous phase observed in the copolymer-rich region might be a reverse bicontinuous (V_2) or reverse micellar cubic (I_2) phase although clear SAXS peaks were not observed. Other intermediate phases (e.g., disordered hexagonal phase) should present anisotropy. I_2 and V_2 phases could be distinguished by dye method.²⁵ Using yellow water-soluble dye (Tartrazine) and red oil-soluble one (Sudan III), it was observed that the water-soluble dye did not penetrate in the isotropic viscous phase of the water/ C_{12}EO_5 / $\text{Si}_{25}\text{C}_3\text{EO}_{3.2}$ system, whereas the oil-soluble dye penetrated in it. From these results, it is considered that the isotropic viscous phase consists of reverse micelles.²⁵

Miscibility of Surfactant and Copolymer in the Liquid Crystalline Phases. To understand the miscibility of silicone copolymer and surfactant in the liquid crystalline phases, we measured the SAXS spectra for water- $\text{Si}_m\text{C}_3\text{EO}_{3.2}$ systems at constant total amphiphile concentration in water ($W_S = 0.7$) as a function of the mixing fraction of copolymer in the total amphiphile. The composition is followed by line B in Figure 1. The SAXS patterns and their corresponding changes in the d values are shown in Figure 4, panels A and B.

At $W_1 = 0$ (100% C_{12}EO_5), a single-phase lamellar liquid crystal is formed. In the $\text{Si}_{5.8}\text{C}_3\text{EO}_{3.2}$ - C_{12}EO_5 system, the interlayer spacing gradually widens or is shifted to lower q values with increasing the copolymer content. This means that the $\text{Si}_{5.8}\text{C}_3$ chain is completely miscible with the surfactant bilayer. On the other hand, for the $\text{Si}_{14}\text{C}_3\text{EO}_{3.2}$ and $\text{Si}_{25}\text{C}_3\text{EO}_{3.2}$ systems, upon small addition of copolymer, another sharp peak is observed at low q values, which is shifted to high q values (d' value decreases) with increase in W_1 , whereas the d values for the C_{12}EO_5 lamellar phase is not changed or even increases slightly. At $W_1 = 0.25$ and 0.3 in the $\text{Si}_{14}\text{C}_3\text{EO}_{3.2}$ and $\text{Si}_{25}\text{C}_3\text{EO}_{3.2}$ systems, respectively, the initial C_{12}EO_5 lamellar phase disappears and all surfactant and copolymer are involved in the formation of the V_1 or H_1 phases. In the middle of composition of copolymer, a macroscopic phase separation takes place because the long hydrophobic chain of the copolymer is not miscible with a thin surfactant bilayer. This result is in good agreement with our previous results.^{14,15} In the copolymer-rich region, the peak position of H_1 phase is shifted to low q values (large d' values) with increasing W_1 as is shown in Figure 4, parts (B)b and (B)c. This means that although the copolymer is not soluble in the surfactant L_α phase, the surfactant dissolves in the copolymer H_1 phase. From the above result, it is considered that the I_1 , H_1 , V_1 , and L'_α phases in Figure 1 are copolymer liquid crystals solubilizing surfactant molecules at the interface of each aggregate.¹⁴

Cloud Temperatures of Water/ C_{12}EO_5 / $\text{Si}_m\text{C}_3\text{EO}_{3.2}$ Systems. The effect of added $\text{Si}_m\text{C}_3\text{EO}_{3.2}$ ($m = 25, 14, 5.8$) on the cloud temperature of C_{12}EO_5 aqueous solution was investigated and the results are shown in Figure 5.

For these experiments the weight fraction of C_{12}EO_5 + $\text{Si}_m\text{C}_3\text{EO}_{3.2}$ in the system, W_S , was kept constant at 2 wt % ($W_S = 0.02$), and the cloud temperature is plotted against the weight fraction of $\text{Si}_m\text{C}_3\text{EO}_{3.2}$ in the total amphiphile, W_1 . Although the purity of $\text{Si}_{5.8}\text{C}_3\text{EO}_{3.2}$ is not as high as the other $\text{Si}_{14}\text{C}_3\text{EO}_{3.2}$ or $\text{Si}_{25}\text{C}_3\text{EO}_{3.2}$, unreacted short-chain poly(ethylene oxide) may not largely influence a cloud temperature since the concentration in water is not high.²⁶ Therefore, the cloud temperature changes are mainly due to changes in W_1 . The cloud temperature for C_{12}EO_5 aqueous solution is 32.1 °C, whereas $\text{Si}_m\text{C}_3\text{EO}_{3.2}$ ($m = 25, 14, 5.8$) are insoluble in water and are essentially silicone oils due to their extremely low f values.^{16,27} Cloud temperature increases with decrease in the aggregation number of the micelles, whereas it decreases by increasing the aggregation number of micelles.²⁸ Besides, the micelle with less aggregation number possesses the positive surfactant layer curvature. Hence, from the results of change of cloud temperature upon addition of additives, it can be estimated that the effect of additives on the aggregation number and the spontaneous surfactant layer curvature of micelles. Like a higher alcohol,^{3,29} the cloud temperature decreases upon addition of $\text{Si}_{5.8}\text{C}_3\text{EO}_{3.2}$. On the contrary, when $\text{Si}_{14}\text{C}_3\text{EO}_{3.2}$ or $\text{Si}_{25}\text{C}_3\text{EO}_{3.2}$ is added to the C_{12}EO_5 aqueous solution, the cloud temperature increases although the silicone chain is elongated. Interestingly, when the more hydrophobic copolymer or the copolymer with the longest hydrophobic chain is mixed with C_{12}EO_5 aqueous solution, the cloud temperature and its maximum value are increased similar to the clouding phenomena observed in nonionic surfactant aqueous solution upon addition of long-chain alkanes, such as C_{12} or C_{16} .³ When conventional lipophilic hydrocarbon chain amphiphiles or polar oils are added to poly-(oxyethylene)-type nonionic surfactant aqueous solution, the cloud temperature always decreases because they are solubilized in the palisade layer and the aggregation number of micelles

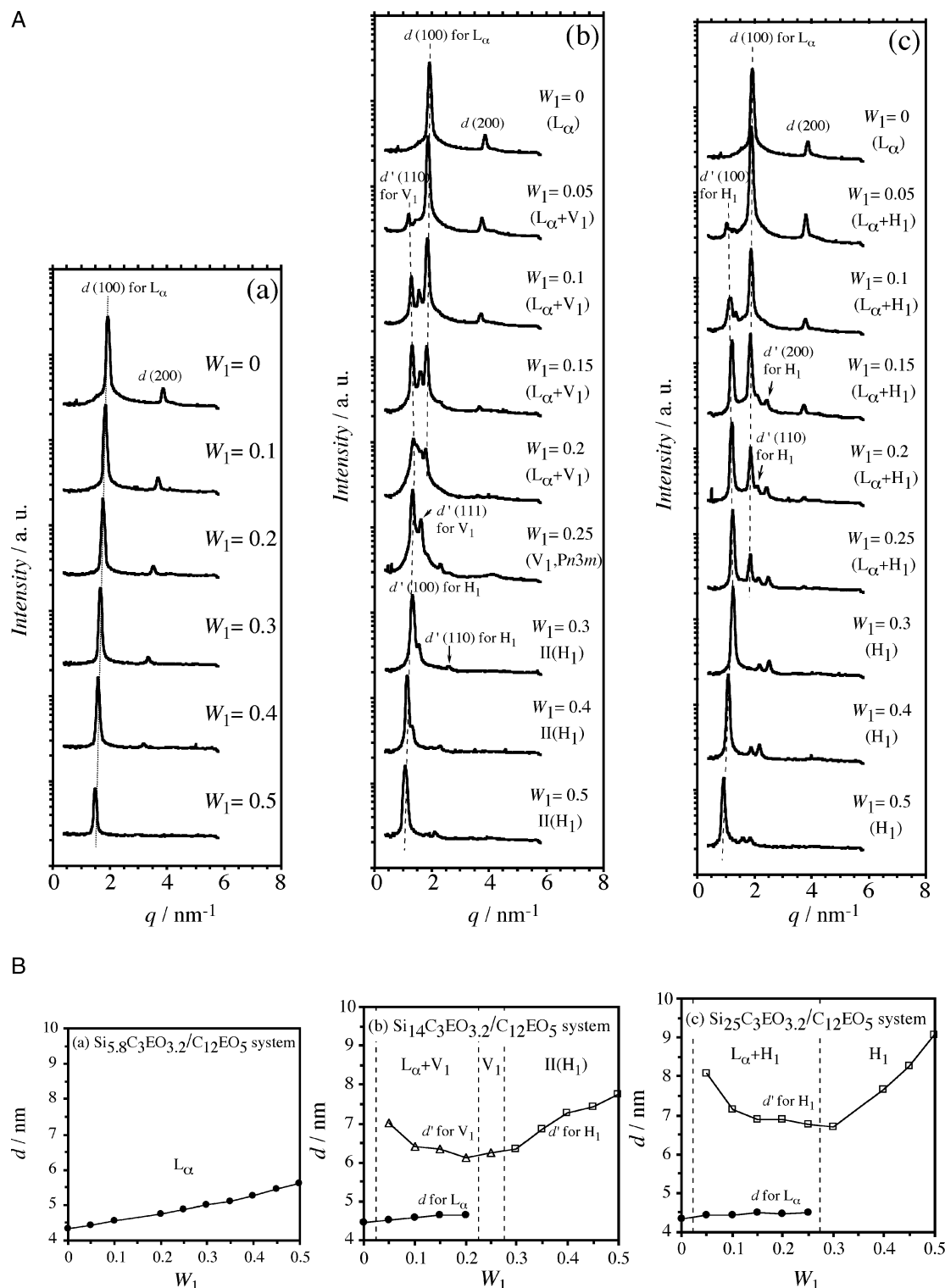


Figure 4. (A) SAXS patterns at constant $W_S = 0.7$ and 25°C . d' represents the copolymer-rich liquid crystalline phase. (a) $\text{Si}_{5.8}\text{C}_3\text{EO}_{3.2}/\text{C}_{12}\text{EO}_5$ system, (b) $\text{Si}_{14}\text{C}_3\text{EO}_{3.2}/\text{C}_{12}\text{EO}_5$ system, and (c) $\text{Si}_{25}\text{C}_3\text{EO}_{3.2}/\text{C}_{12}\text{EO}_5$ system. (B) Change in d values with the weight fraction of copolymer in the mixture (W_1) at 25°C . The mixture (total amphiphile) concentration in the system is fixed at 70 wt % ($W_S = 0.7$). ●: d values for C_{12}EO_5 -rich L_α phase, and △, □: d values for $\text{Si}_m\text{C}_3\text{EO}_{3.2}$ -rich V_1 and H_1 phases, respectively.

increases. In this case, the surfactant layer curvature of micelles becomes less positive, because the hydrophilic chain is very short. The hydrophobic volume of $\text{Si}_{5.8}\text{C}_3\text{EO}_{3.2}$ is approximately $0.84 \text{ nm}^3/\text{chain}$, and it corresponds approximately to the volume of a C_{28} chain. Hence, the decrease in the cloud temperature upon addition of $\text{Si}_{5.8}\text{C}_3\text{EO}_{3.2}$ is similar to that found in conventional amphiphiles or polar oils. The hydrophobicity of $\text{Si}_m\text{C}_3\text{EO}_{3.2}$ increases with increasing the hydrophobic chain,

and it is then expected that the surfactant layer curvature would be less positive upon addition of longer-chain silicone amphiphiles. However, the experimental fact is opposite to this prediction. In the next section, we will investigate the changes in the micellar shape more in detail.

Micellar Structure. The clouding phenomenon of poly-(oxyethylene)-type nonionic surfactant solution is related to the dehydration of the EO chain.³⁰ As a result, the surfactant layer

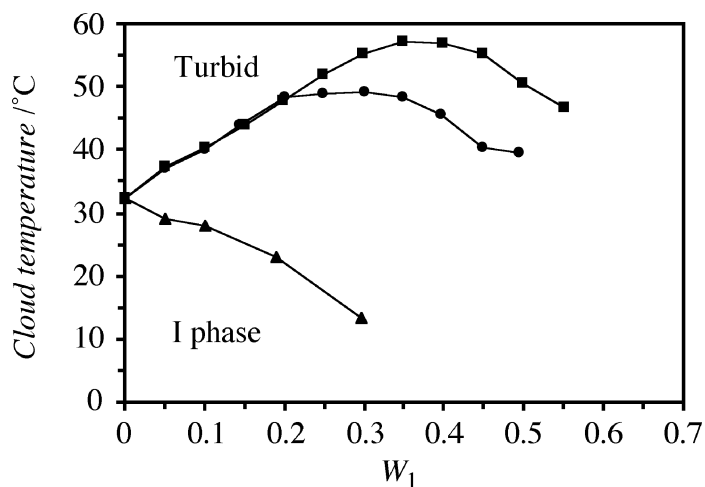


Figure 5. Cloud temperatures for $\text{Si}_m\text{C}_3\text{EO}_{3.2}/\text{C}_{12}\text{EO}_5$ aqueous systems as a function of the weight fraction of $\text{Si}_m\text{C}_3\text{EO}_{3.2}$ in the mixture, W_1 at constant $W_S = 0.02$. ■: $m = 25$, ●: $m = 14$, ▲: $m = 5.8$.

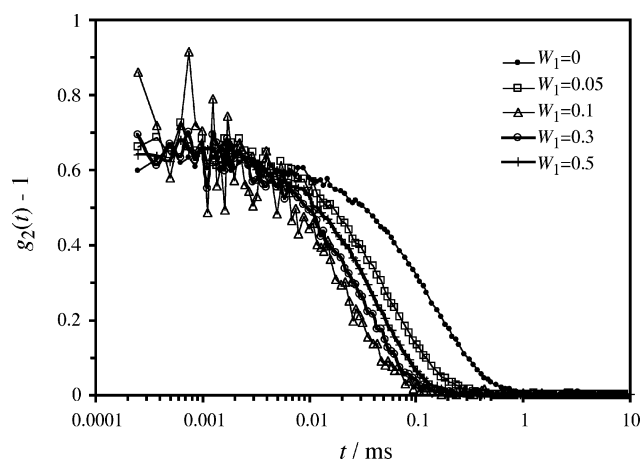


Figure 6. Change of the correlation functions, $g_2(t)-1$, at different W_1 in a water/ $\text{C}_{12}\text{EO}_5/\text{Si}_{25}\text{C}_3\text{EO}_{3.2}$ system at 25 °C. The mixture concentration is fixed at 0.5 wt % ($W_S = 0.005$). The measurement angle is 90°.

curvature decreases, the aggregation number of micelle increases and eventually, the surfactant is separated from water. The change of micellar size was investigated with increase in copolymer content at a fixed mixture concentration, $W_S = 0.005$ and 25 °C. The observed correlation functions, $g_2(t)-1$, are shown in Figure 6. Although $g_2(t)-1$ does not reach the theoretical value of 1 due to the performance of the instrument, it is clear that $g_2(t)-1$ is shifted to short times with increase in copolymer content up to $W_1 = 0.1$, and then moves to longer times for $W_1 \geq 0.3$. From this tendency, it can then be said that by adding copolymer large surfactant micelles change first to small micelles, and then again they become larger upon addition of more amounts copolymer.

The experimental correlation functions were analyzed by the CONTIN program and the results are shown in Figure 7.

It can be seen that the distribution of hydrodynamic radii, $A(R_H^{\text{app}})$, for $W_1 = 0$ is relatively wide. Upon addition of copolymer, this distribution becomes somehow narrow. In general, it is expected that spherical micelles have homogeneous radii, whereas the polydispersity in the case of nonspherical micelles, as for example, rodlike or ellipsoid micelles, is much higher. Thus, from this simple observation, it is suggested that a rod-sphere transition of the micellar shape takes place upon addition of copolymer.

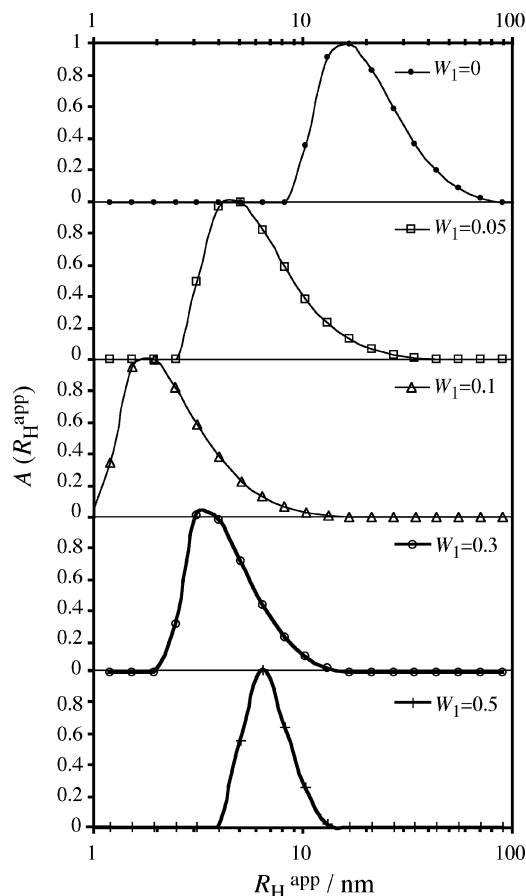


Figure 7. Distribution of the apparent hydrodynamic radii, R_H^{app} , at different W_1 in a water/ $\text{C}_{12}\text{EO}_5/\text{Si}_{25}\text{C}_3\text{EO}_{3.2}$ system at 25 °C. The mixture concentration is fixed at 0.5 wt % ($W_S = 0.005$). The measurement angle is 90°.

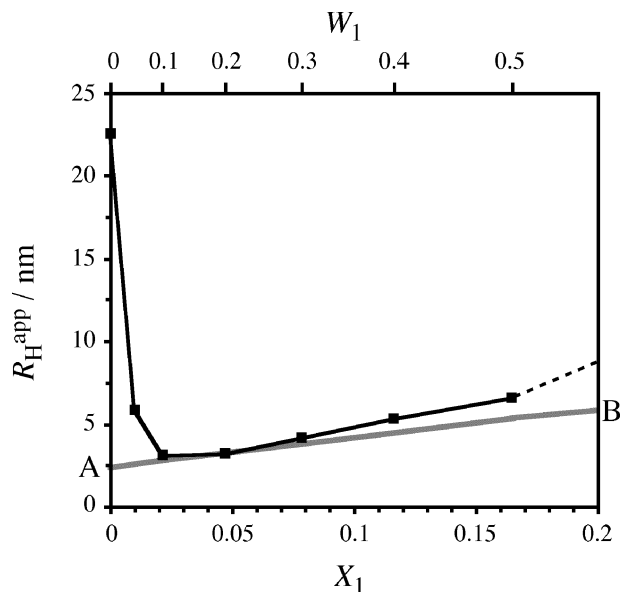


Figure 8. Change of the apparent hydrodynamic radius, R_H^{app} , as a function of the copolymer mole fraction, X_1 , in a water/ $\text{C}_{12}\text{EO}_5/\text{Si}_{25}\text{C}_3\text{EO}_{3.2}$ system at 25 °C. The line A–B represents the calculated values r on the spherical model.

To confirm this, we calculated the apparent hydrodynamic radii (R_H^{app}) of the aggregates formed in the C_{12}EO_5 – $\text{Si}_{25}\text{C}_3\text{EO}_{3.2}$ system, and the results are shown in Figure 8.

The low, high horizontal and vertical axes represent X_1 , W_1 and R_H^{app} , respectively. X_1 is the mole fraction of $\text{Si}_{25}\text{C}_3\text{EO}_{3.2}$ in

the C₁₂EO₅/Si₂₅C₃EO_{3.2} mixture. The concentration dependence of R_H^{app} can be described by the following equation:

$$R_H^{\text{app}} = \frac{R_H}{1 + AC} \quad (10)$$

where R_H is the hydrodynamic radius at infinite dilute, A is a constant with a value of 1.56 for the hard-sphere model,^{31,32} and C is the concentration of particles (micelles) in the system. In a real case, it has also to be considered that A should include the effect of hydrated water in the poly(oxyethylene) chain. Approximately four water molecules are hydrated in one poly(oxyethylene) chain as measured by NMR^{33,34} and dielectric relaxation spectroscopy.³⁵ Even if hydrated water molecules are taken into account, the difference between R_H and R_H^{app} is less than 1.5 wt %. Thus, in our experiments with very diluted micellar solutions ($W_S = 0.005$), the R_H^{app} measured is nearly equivalent to R_H .

For the following calculations, we assume that all surfactants and copolymers are involved in the formation of the mixed spherical micelles, in which the effective cross sectional areas of surfactant and copolymer are constant. The hydrophobic volumes are also constant. a_S for C₁₂EO₅ ($a_{S,S}$) taken from its L_α phase is 0.44 nm², and a_S for Si₂₅C₃EO_{3.2} ($a_{S,P}$) = 0.70 nm².¹⁶ The volumes of hydrophobic part of copolymer¹⁶ and surfactant^{2,18} are $V_{L,P} = 3.29$ nm³ and $V_{L,S} = 0.357$ nm³, respectively. For a spherical model of the micelles, the radius of the hydrophobic part, r , is calculated from the surface area, A_L , and the volume, V_{ML} , of the hydrophobic parts of the mixed micelles as follows:

$$r = \frac{3V_{ML}}{A_L} \quad (11)$$

and

$$A_L = N_{\text{agg}}\{X_1 a_{S,P} + (1 - X_1) a_{S,S}\} \quad (12)$$

$$V_{ML} = N_{\text{agg}}\{X_1 V_{L,P} + (1 - X_1) V_{L,S}\} \quad (13)$$

where N_{agg} is the surfactant and copolymer total aggregation number. Change of r as a function of X_1 for this model is shown as A–B line in Figure 8. It can be observed that in the copolymer-rich region, from $W_1 = 0.1 \sim 0.5$, the R_H^{app} value is in relatively good agreement with the radius r calculated from the spherical model, whereas R_H^{app} is vastly separated from r in the surfactant-rich region ($W_1 < 0.1$). As discussed above, this disagreement can be attributed to the shape of the micelles. We assume then that the C₁₂EO₅ forms prolate ellipsoidal micelles at $W_1 = 0$. The hydrodynamic radius for a prolate ellipsoid of semiminor axis a and semimajor b is given by^{36,37}

$$R_H = \frac{b(1 - a^2/b^2)^{1/2}}{\ln \left[\frac{1 + (1 - a^2/b^2)^{1/2}}{a/b} \right]} \quad (14)$$

The semiminor axis, a , is chosen to be 2.67 nm, which includes the extended length of C₁₂ (1.67 nm)¹⁸ and EO₅ (~1 nm).³⁸ From the experimental results, the semimajor axis b varies from approximately 5 (at $W_1 = 0.1$) to 100 nm (pure surfactant) as is shown in Figure 9.

Bernheim-Groswasser et al. directly observed the micellar shape of 0.5 wt % C₁₂EO₅ aqueous solution at 18 °C and 29 °C by cryo-TEM and reported that 50–100 nm threadlike micelles

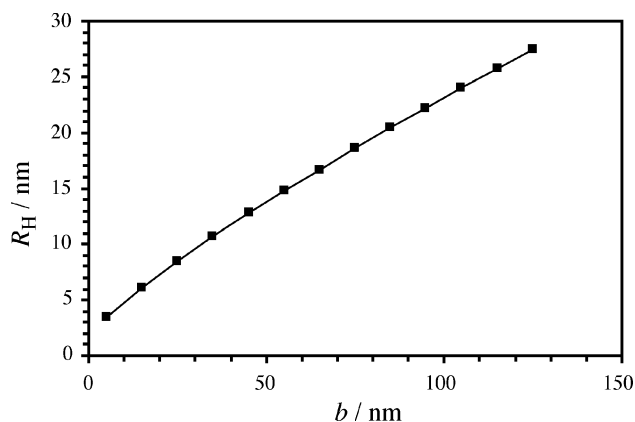


Figure 9. Change of R_H with the semimajor axis b at constant the semiminor axis, $a = 2.67$ in eq 14.

exist between 18 °C and 29 °C.³⁹ It is also confirmed that C₁₂EO₅ forms rodlike micelle in water by using DLS⁴⁰ or NMR⁴¹ experiments. All of these results support our hypothesis that rodlike micelles are formed in the surfactant-rich region, and that, upon addition of copolymer, the rod-sphere transition in micellar shape takes place.

So far, in previous works (see, for example, refs 3 and 29), it has been considered that the cloud temperature for the nonionic surfactant decreases upon addition of a hydrophobic amphiphile, because the hydrophobic amphiphile forms a mixed microinterface with the nonionic surfactant and changes the mixed interface curvature toward negative. However, we have seen that when an amphiphilic block copolymer with a large hydrophobic chain, such as Si₂₅C₃ and Si₁₄C₃, is mixed with the nonionic surfactant, the chain tends to make an oil pool in the core of the micelle to minimize the surface area, leading to a change in the curvature toward more positive at the mixed interface. As a result, the cloud temperature for the nonionic surfactant solution increases upon addition of the amphiphilic block copolymer containing a bulky hydrophobic chain.

Conclusions

The phase behaviors of mixtures of C₁₂EO₅ and hydrophobic Si_mC₃EO_{3.2} in water were discussed. In the ternary water/C₁₂EO₅/Si₂₅C₃EO_{3.2} system, a rich phase behavior was observed with the formation of I₁, H₁ and V₁ phases. It has also been observed that these liquid crystals are essentially copolymer liquid crystals (I₁, H₁, and V₁ phases). Si₂₅C₃EO_{3.2} and Si₁₄C₃EO_{3.2} cannot be dissolved into the C₁₂EO₅ bilayer and phase separation between surfactant and copolymer-rich phases takes place.

Consequently, hydrophobic Si_mC₃EO_{3.2} copolymers have a dual behavior in changing the shape of self-assemblies. If the hydrophobic chain is very long, the silicone copolymer does not dissolve in the surfactant lamellar phase, in which the bilayer has no capacity to incorporate the bulky silicone chain. But, they form mixed aggregates in the copolymer-rich region. The short hydrophobic chain is located at the mixed interface and the surfactant–copolymer layer curvature tends to change to less positive. If the hydrophobic chain is large enough, it makes an oil pool inside the aggregate and it tends to change the layer curvature more positive like what occurs solubilizing saturated hydrocarbons.

In the dilute region, the same phenomenon is observed. Upon addition of Si₂₅C₃EO_{3.2} or Si₁₄C₃EO_{3.2}, the cloud temperature for C₁₂EO₅ aqueous solution is increased, whereas it is decreased upon addition of Si_{5.8}C₃EO_{3.2}. Si_{5.8}C₃EO_{3.2} makes the surfactant

layer curvature negative. On the contrary, $\text{Si}_{14}\text{C}_3\text{EO}_{3.2}$ and $\text{Si}_{25}\text{C}_3\text{EO}_{3.2}$ make an oil pool inside the micelle leading to a rod to sphere transition in the micellar shape.

Acknowledgment. The author gratefully acknowledges helpful discussions with Dr. T. Sato. This work was supported by Core Research for Evolutional Science and Technology (CREST) of JST Corporation.

References and Notes

- (1) Kunieda, H.; Umizu, G.; Aramaki, K. *J. Phys. Chem. B* **2000**, *104*, 2005.
- (2) Kunieda, H.; Ozawa, K.; Huang, K.-L. *J. Phys. Chem. B* **1998**, *102*, 831.
- (3) Kunieda, H.; Horii, M.; Koyama, M.; Sakamoto, K.; *J. Colloid Interface Sci.* **2001**, *236*, 78.
- (4) Hoffmann, H.; Ulbricht, W.; *J. Colloid Interface Sci.* **1989**, *129*, 388.
- (5) Nagarajan, R.; Ruckenstein, E. *Langmuir* **1997**, *7*, 22934.
- (6) Menge, U.; Lang, P.; Findenegg, G. H. *J. Phys. Chem. B* **1999**, *103*, 5768.
- (7) Menge, U.; Lang, P.; Findenegg, G. H. *Coll. Surf. Sci. A* **2000**, *163*, 81.
- (8) Menge, U.; Lang, P.; Findenegg, G. H.; Strunz, P. *J. Phys. Chem. B* **2003**, *107*, 1316.
- (9) Li, X.; Kunieda, H. *Langmuir* **2000**, *16*, 10092.
- (10) Jin-Feng; Aramaki, K.; Ogawa, A.; Katsuragi, T.; Kunieda, H.; *Colloid Polym. Sci.* **2001**, *279*, 92.
- (11) Owen, M. *J. Ind. Eng. Chem., Prod. Res. Dev.* **1980**, *19*, 97.
- (12) Hill, R. M.; He, M.; Lin, Z.; Davis, H. T.; Scriven, L. E. *Langmuir* **1993**, *9*, 2789.
- (13) Zheng, Y.; Davis, H. T. *Langmuir* **2000**, *16*, 6453.
- (14) Kunieda, H.; Uddin, Md. H.; Furukawa, H.; Harashima, A. *Macromolecules* **2001**, *34*, 9093.
- (15) Kunieda, H.; Kaneko, M.; López-Quintela, M. A.; Tsukahara, M.; *Langmuir* **2004**, *20*, 2164.
- (16) Kunieda, H.; Uddin, Md. H.; Horii, M.; Furukawa, H.; Harashima, A. *J. Phys. Chem. B* **2001**, *105*, 5419.
- (17) Kunieda, H.; Taoka, H.; Iwanaga, T.; Harashima, A. *Langmuir* **1998**, *14*, 5113.
- (18) Tanford, C. *J. Phys. Chem.* **1972**, *76*, 3020.
- (19) Huang, K. L.; Shigeta, K.; Kunieda, H. *Prog. Colloid Polym. Sci.* **1982**, *110*, 171.
- (20) Stepánek, P. In *Dynamic Light Scattering*; Brown, W., Ed.; Oxford University Press: New York, 1993.
- (21) Mitchell, D. J.; Tiddy, G. J. T.; Waring, L.; Bostock, T.; McDonald, M. P. *J. Chem. Soc., Faraday Trans. 1* **1983**, *79*, 975.
- (22) Strey, R.; Schomäcker, R.; Roux, D.; Nallet, F.; Olsson, U. *J. Chem. Soc., Faraday Trans. 1* **1990**, *86*, 2253.
- (23) Thomas, E. L.; Alward, D. B.; Kinning, D. J.; Martin, D. C.; Handlin, D. L.; Fetters, L. J. *Macromolecules* **1986**, *19*, 2197.
- (24) Hasagawa, H.; Tanaka, H.; Yamasaki, K.; Hashimoto, T. *Macromolecules* **1987**, *20*, 1641.
- (25) Kunieda, H.; Aramaki, K.; Izawa, T.; Kabir, Md. H.; Sakamoto, K.; Watanabe, K. *J. Ore Sci.* **2003**, *52*, 429.
- (26) Iwanaga, T.; Suzuki, M.; Kunieda, H.; *Langmuir* **1998**, *14*, 5775.
- (27) Kitahara, A. *J. Phys. Chem.* **1965**, *69*, 2788.
- (28) Shigeta, K.; Olsson, U.; Kunieda, H.; *Langmuir* **2001**, *17*, 4717.
- (29) Kim, E. J.; Shah, D. O. *J. Phys. Chem. B* **2003**, *107*, 8689.
- (30) Karlström, G. *J. Phys. Chem.* **1985**, *89*, 4962.
- (31) Pusey, P. N.; Tough, R. J. A. In *Dynamic Light Scattering*; Pecora, R., Ed.; Plenum Press: New York, 1985.
- (32) Fijnaut, H. M. *J. Chem. Phys.* **1981**, *74*, 6857.
- (33) Nilsson, P. G.; Lindman, B. *J. Phys. Chem.* **1983**, *87*, 4756.
- (34) Klose, G.; Eienblätter, St; Galle, J.; Islamov, A.; Dietrich, U. *Langmuir* **1995**, *11*, 2889.
- (35) Sato, T.; Hossain, Md. K.; Acharya, D. P.; Glatter, O.; Chiba, A.; Kunieda, H. *J. Phys. Chem. B* accepted.
- (36) Missel, P. J.; Mazer, N. A.; Benedek, G. B.; Young, C. Y.; Carey, M. C. *J. Phys. Chem.* **1980**, *84*, 1044.
- (37) Porte, G.; Appell, J. *J. Phys. Chem.* **1981**, *85*, 2511.
- (38) Kalyanasundaram, K.; Thomas, J. K. *J. Phys. Chem.* **1976**, *80*, 1462.
- (39) Bernheim-Groswasser, A.; Wachtel, E.; Talmon, Y. *Langmuir* **2000**, *16*, 4131.
- (40) Kato, T.; Anzai, S.; Takano, S.; Seimiya, T. *J. Chem. Soc., Faraday Trans. 1* **1989**, *85*, 2499.
- (41) Nilsson, P. G.; Wennerström, H.; Lindman, B. *J. Phys. Chem.* **1983**, *87*, 1377.